

Threshold Region Performance of Multi-Carrier Maximum Likelihood Direction of Arrival Estimator

Francesca Filippini*, Fabiola Colone*, Antonio De Maio⁺

* Dept. of Information Engineering, Electronics and Telecommunications (DIET),
Sapienza University of Rome, Via Eudossiana, 18 - 00184 Rome, Italy

⁺ Dip. di Ingegneria Elettrica e delle Tecnologie dell'Informazione,
Universita degli Studi di Napoli "Federico II", via Claudio 21, I-80125 Napoli, Italy

Abstract — This paper addresses performance characterization of a direction of arrival (DoA) estimator in the low signal-to-noise-ratio (SNR) region. The case of a sensor array simultaneously collecting signals emitted at multiple carrier frequencies by a single source is considered. A maximum likelihood (ML) approach is used as a reference method for DoA estimation and its accuracy is characterized in terms of mean square error (MSE). It is well known that, for SNR values included in the so-called threshold region, the DoA estimation accuracy decreases rapidly, due to the presence of outliers. This effect can be possibly mitigated when multiple frequency channels are jointly exploited. However, the capability to predict this performance degradation is fundamental either for assessing the robustness of an existing sensor or for supporting its design. Therefore, the scope of this paper is to introduce appropriate approximations to the MSE of a multi-frequency ML DoA estimator in order to provide a reliable characterization of its performance in the threshold region. Two models for the source signals are considered and separately discussed, namely the deterministic (or conditional) and stochastic (or unconditional). An extensive simulated analysis is reported to prove the tightness of the approximations and to characterize the benefits stemming from the exploitation of signals emitted at multiple carriers.

Index Terms — array signal processing, direction of arrival, maximum likelihood, estimation accuracy, threshold region.

I. INTRODUCTION

A. Overview

Direction of arrival (DoA) estimation of narrow-band signals is a key problem in sensor array signal with a variety of application fields, such as radar, sonar, mobile communications, etc. The conspicuous interest attracted by this issue is testified by the amount of research literature dedicated to the topic, see e.g. [1] and the references therein. A variety of advanced estimation methods has been proposed and their performances have been extensively studied [2]-[10].

However, the majority of studies published over the years addressed the problem of characterizing the performance of DoA estimators under asymptotic assumptions, where asymptotic generally refers to either a high number of samples or high signal-to-noise ratio (SNR) regime, [5]-[8].

Nevertheless, in many practical applications, such conditions are unlikely to be continuously guaranteed. This is the case of passive location systems, where the object of the location task could be an emitting source [11]-[13] or a target that backscatters a signal of opportunity, as in passive radar [14]-[16] or passive sonar [17] systems. The passive nature of such systems intrinsically limits the possibility to fully control the performance for any target of interest. Specifically, the DoA estimation accuracy largely depends on the power level and the transmission rate of either the emitting source, in one-way propagation systems, or the illuminator of opportunity, in two-way propagation systems. These parameters cannot be directly controlled by the system designer. Therefore it is not unlikely that the aforementioned systems operate in the low SNR regime where accurate angular localization might represent a challenging task. This is especially true when a limited number of receiving sensors is employed in order to limit the system complexity.

As it is well known, at low SNR values, the estimation accuracy of a nonlinear DoA estimator rapidly deviates from its asymptotic performance, experiencing the so-called threshold effect [8]-[10]. This effect is qualitatively shown in Fig. 1, where the mean square error (MSE) is reported versus the SNR: three regions can be identified, referred to as *no information region* (as $SNR \rightarrow 0$), *threshold region* and *asymptotic region* (as $SNR \rightarrow \infty$). The Cramér-Rao lower bound (CRB) [8], in dashed red, correctly describes the estimator performance in the asymptotic region, but it is not able to predict the estimator performance for low SNR values. In fact, while the CRB essentially depends on the local errors around the true value, the threshold effect is due to outliers, namely global estimation errors that occur due to an actual estimate outside the mainlobe of the objective function. This issue has been addressed in the open literature by several authors [8],[18]-[23]. A number of lower bounds has been proposed, accounting for the global errors contribution to the overall MSE, see e.g. the Barankin bound [21], the Bayesian CRB [8],[18], the Ziv-Zakai bound [23].

With reference to the problem under consideration, a very tight bound has been provided in [19], which is able to predict the threshold behaviour of a maximum likelihood (ML) DoA

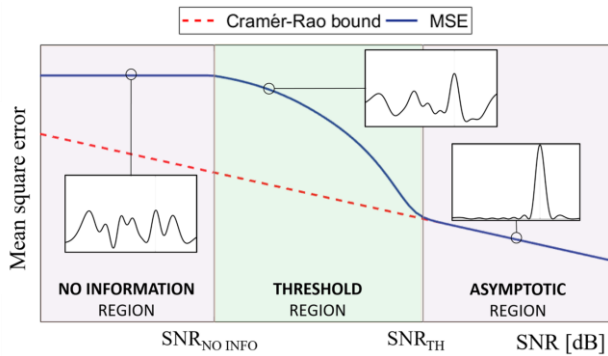


Fig. 1 Qualitative behavior of the MSE versus the SNR for nonlinear DoA estimation. Three different operative regions are distinguished.

estimator for an array of sensors, receiving narrow-band signals from far-field emitters.

It is based on some ideas presented in [9] and [10]. Basically, the MSE is splitted into two parts, the former coming from local errors obtained when the estimates are close to the true value, and the latter due to outliers.

B. Contribution

In this paper, we elaborate on the achievements in [19] and deal with the case of a multiple frequency (MF) ML DoA estimator that exploits a non-uniform linear array receiving multiple signals simultaneously emitted at different carrier frequencies. Frequency diversity has been considered in sensor array processing with various objectives, using both coherent and non-coherent integration approaches, in several applications. They include, for instance, frequency diverse array (FDA) [24], frequency diversity based multiple-input multiple-output (MIMO) [25],[26], and multi-frequency co-prime arrays [27].

We refer to DoA estimation based on the non-coherent exploitation of signals received at multiple carriers as a mean to mitigate the problem of angular ambiguities in arrays enjoying a limited number of channels. This idea is based on recognizing the change in the array grating lobe pattern that results from the change of frequency and it finds application in several scenarios [28].

Among the most interesting, we mention DoA estimation of single source that transmits signals on multiple carriers, either simultaneously or with rapid frequency hopping. For instance, this is the case of remotely piloted unmanned aerial vehicles (UAV) carrying RF emitting devices. Since the considered multi-carrier sources should not necessarily share the same transmitting antenna, possible scenarios of application also encompass the case of multiple emitters carried by the same platform, e.g. ships or aircrafts [29]. Another very interesting application context is offered by multi-band radar and sonar systems that aim at localizing targets backscattering signals emitted on multiple frequency channels by either one (i.e. mono-/bi-static configuration) or several transmitters (i.e. multistatic configuration).

This scenario also embraces the case of passive radar systems exploiting co-located or geographically distributed broadcast transmitters as illuminators of opportunity [16].

The purpose of this paper is to provide a reliable performance characterization of the MF ML estimator in the threshold region. To this end, we exploit the same approach adopted in [19] and use some recent results from the theory of indefinite quadratic forms in Gaussian random variables [30] to evaluate the probability of outlier for the considered estimator. With reference to the source signal, two different models are considered, namely the deterministic and the stochastic, often referred to as conditional model assumption (CMA) and unconditional model assumption (UMA), respectively.

The capability to predict jointly the threshold and asymptotic performance of the MF ML DoA estimator via the expressions derived in this paper enables a fair comparison between different array configurations without resorting to time-consuming Monte Carlo simulations.

Also the benefits of the multi-carrier approach can be easily characterized based on the developed tool. Finally the results derived in this work could also be used to address robust design optimization of the sensor array layout.

C. Outline of the Paper

The paper is organized as follows. We introduce the signal model and the MF ML DoA estimator in Section II. The approximations adopted for the MSE and the probability of outlier are illustrated in Section III, along with the results obtained in [19]. In Section IV and V we develop theoretical expressions for the probability of outlier with reference to the more general multi-carrier case, under deterministic and stochastic signal model assumptions, respectively.

In both sections, the results of Monte Carlo simulations are provided to support the accuracy of the obtained expressions. The simulated analysis is further extended in Section VI where the validity of the adopted approximations is verified in terms of MSE and the threshold region performance of the MF ML estimator is investigated for various system configurations. Finally, some conclusions are drawn in Section VII.

Notation

\hat{u}_0	estimate of u_0
$(\cdot)^T$	transpose
$(\cdot)^*$	conjugate
$(\cdot)^H$	Hermitian or conjugate transpose
$\Pr[\cdot]$	probability
$E[\cdot]$	expectation
\mathbf{I}_N	$N \times N$ identity matrix
$\text{Tr}(\cdot)$	trace
$\text{Re}(\cdot), \text{Im}(\cdot)$	real and imaginary parts
$\det(\cdot)$	determinant
\otimes	Kronecker product

II. SIGNAL MODEL AND MULTI-CARRIER MAXIMUM LIKELIHOOD DOA ESTIMATOR

Let us consider a K -dimensional linear array¹, with $K \geq 2$ identical spatial channels, receiving narrowband signals at N different carrier frequencies. This array is employed to estimate the DoA u_0 of a multi-frequency source when measurements are severely corrupted by noise.

Assuming that a single source is present, the complex array output (after down-conversion, filtering and sampling) for the l -th frequency channel can be arranged into the K -dimensional column vector

$$\mathbf{x}_l(t) = A_l(t)\mathbf{s}_l(u_0) + \mathbf{n}_l(t) \quad (1)$$

$(l = 0, \dots, N-1, \quad t = 0, \dots, M_l-1)$

where

- $A_l(t)$ ($l = 0, \dots, N-1$) is the complex baseband source signal. Depending on the application, it can represent the samples of the signal emitted by the source to be localized or the complex amplitude of the target backscattering in response to the signal of opportunity emitted at the l -th frequency channel. We model $A_l(t)$ ($l = 0, \dots, N-1, t = 0, \dots, M_l-1$) as unknown parameters and handle them according to the stochastic and the deterministic framework.
- $\mathbf{s}_l(u_0)$ is the target steering vector and accounts for the array response from the target DoA. For a linear array composed by K elements at positions d_k ($k = 0, \dots, K-1$) measured with respect to a generic phase reference location along the array, it is

$$\mathbf{s}_l(u_0) = \left[e^{-j\frac{2\pi}{\lambda_l}d_0u_0} \quad \dots \quad e^{-j\frac{2\pi}{\lambda_l}d_{K-1}u_0} \right]^H \quad (2)$$

where $u_0 = \sin(\theta_0)$ is the target DoA measured relative to the array boresight and λ_l is the l -th wavelength.

- \mathbf{n}_l is a K -dimensional vector that collects the additive noise samples at the receiving sensors. The noise is assumed to be a spatially white zero-mean complex Gaussian process with unknown mean square value σ_n^2 , independent of the source signal. It is further supposed that the noise contributions at different frequency channels are statistically independent and identically distributed (i.i.d.).
- M_l is the number of space snapshots available for the signal at the l -th carrier frequency and it is assumed known. In the general case, a different number of snapshots might be available for the different frequency channels and their total number is denoted by $L = \sum_{l=0}^{N-1} M_l$.

Under the above hypotheses, the ML estimate of the DoA u_0 [8] is found by jointly maximizing the likelihood function with respect to $A_l(t)$ ($l = 0, \dots, N-1, \quad t = 0, \dots, M_l-1$) and u_0 , yielding

$$\hat{u}_0 = \underset{u}{\operatorname{argmax}} \{V(u)\} \quad (3)$$

where $u \in [-u_{MAX}, u_{MAX}]$ with $u_{MAX} = 1$ if the non-ambiguous angular sector is $[-\pi, \pi]$ and $V(u)$ is the concentrated ML objective function

$$V(u) = \sum_{l=0}^{N-1} \sum_{t=0}^{M_l-1} |\mathbf{s}_l^H(u) \mathbf{x}_l(t)|^2 \quad (4)$$

In the absence of noise, this function is proportional to the weighted sum of the estimated array beampattern amplitudes computed at different carrier frequencies, i.e. $b_l(u) = |\mathbf{s}_l^H(u) \mathbf{s}_l(u_0)|^2$. This is a direct consequence of the used model for the complex amplitudes $A_l(t)$ across multiple frequency channels that does not enable the coherent summation of the results obtained at different carrier frequencies.

The asymptotic properties of the ML estimator are well known, whereas its performance in the threshold region has been characterized only in specific cases. In [19] an suitable approximation to the MSE of the ML estimator is provided for a non-uniform linear array exploiting a single carrier frequency case, i.e. for $N = 1$.

The purpose of this work is to extend the analysis of [19] to the multi-carrier ($N > 1$) scenario in order to provide a reliable characterization of the ML estimator performance close to the threshold when multiple frequency channels are employed. We observe that this extension is not straightforward as the exploitation of multiple signals emitted at multiple carriers has a non-trivial impact on the threshold SNR value. In fact it simultaneously affects (i) the useful signal energy thanks to the increase of the number of snapshots, and (ii) the multi-frequency beampattern characteristics thanks to the diversity conveyed by multiple frequency channels, especially when the corresponding carriers are widely separated.

III. APPROXIMATION OF THE MSE AND PROBABILITY OF OUTLIER

In this Section, we briefly summarize the approach proposed in [19] to obtain an approximate expression for the MSE of the ML estimator in the threshold region, as it represents the starting point adopted in this paper.

¹ Whilst the model in (1) as well as the specific results reported in the manuscript have been developed for the case of linear arrays, the proposed methodology for DoA estimation performance analysis in the low SNR region still can be reframed to the case of a planar array, provided that a bi-dimensional (azimuth/elevation) domain is considered for the search.

The MSE is split into two parts, one coming from small errors obtained when the estimates are close to the true value, and the other due to outliers. The total probability theorem implies that the MSE can be written as

$$E[(\hat{u}_0 - u_0)^2] = \Pr\{\text{no outlier}\} E[(\hat{u}_0 - u_0)^2|\text{no outlier}] + \Pr\{\text{outlier}\} E[(\hat{u}_0 - u_0)^2|\text{outlier}] \quad (5)$$

We recall that the probability of outlier P_0 is the probability of the event that, due to the presence of noise, the global maximum in the likelihood function is outside the mainlobe of the objective function. Close to the threshold region, outliers will tend to concentrate around the sidelobe peaks of the beampattern. Therefore, considering the function in (4) at the sidelobe peaks, $V(u_m)$ ($m = 1, \dots, N_p$), and resorting to the union bound [31] we can approximate P_0 as

$$P_0 \approx \sum_{m=1}^{N_p} P_m = \sum_{m=1}^{N_p} \Pr\{V(u_m) > V(u_0)\} \quad (6)$$

Notice that the positions u_m of the nominal sidelobe peaks in (6) are identified based on the theoretical (noise-free) MF beampattern corresponding to (4). This can be written as

$$V_{theo}(u) = \sigma_n^2 \sum_{l=0}^{N-1} M_l \text{SNR}_l b_l(u) \quad (7)$$

where SNR_l is the SNR available at the single antenna element, for the single snapshot received at the l -th frequency channel, and its explicit expression will be provided in the subsequent sections with reference to each adopted signal model. The numbering of the sidelobe peaks positions is defined so that u_0 is the position of the mainlobe peak and u_m , $m = 1, \dots, N_p$ are the positions of the N_p sidelobe peaks of the resulting MF beampattern. The individual probabilities P_m will be referred to as the pairwise error probabilities, borrowing this terminology from communication theory [31].

Exploiting (6), the MSE approximation for the considered ML estimator is written as

$$E[(\hat{u}_0 - u_0)^2] \approx \left[1 - \sum_{m=1}^{N_p} P_m \right] \cdot \text{CRB} + \sum_{m=1}^{N_p} P_m (u_m - u_0)^2 \quad (8)$$

where the CRB is used as a good predictor of the small errors of the MSE in the asymptotic region.

Notice that this approximate expression is quite general and applies also to the case under consideration since the number N of frequency channels, the corresponding wavelengths, and the number M_l of snapshots available at the l -th carrier frequency will largely affect the pairwise error probabilities, the position of sidelobe peaks, and the CRB.

A closed form expression for the pairwise error probabilities P_m ($m = 1, \dots, N_p$) has been derived in [19] for the case $N = 1$, and two different signal models, namely the deterministic (or conditional) and the stochastic (or unconditional).

In the former case, the amplitudes $A(t)$ ($t = 0, \dots, M - 1$) are assumed to be deterministic (but unknown) complex values whereas in the latter situation, the signal is assumed to be a stationary, temporally white, zero-mean, complex Gaussian process. We report the derived expressions here for ease of reference.

1) Deterministic Signal Model (or Conditional Model Assumption – CMA)

$$P_m = Q \left(\sqrt{\frac{S}{2} (1 - \sqrt{1 - |g_m|^2})}, \sqrt{\frac{S}{2} (1 + \sqrt{1 - |g_m|^2})} \right) - e^{-\frac{S}{2}} \left\{ I_0 \left(\frac{|g_m|S}{2} \right) - \frac{1}{2^{2M-1}} I_0 \left(\frac{|g_m|S}{2} \right) \sum_{p=0}^{M-1} \binom{2M-1}{p} - \frac{1}{2^{2M-1}} \sum_{p=1}^{M-1} I_p \left(\frac{|g_m|S}{2} \right) \times \left[\left(\frac{1 + \sqrt{1 - |g_m|^2}}{|g_m|} \right)^l - \left(\frac{1 - \sqrt{1 - |g_m|^2}}{|g_m|} \right)^l \right] \sum_{k=0}^{M-1-p} \binom{2M-1}{k} \right\} \quad (9)$$

where

$$Q(\alpha, \beta) = \int_{\beta}^{\infty} t e^{-\frac{(t^2 + \alpha^2)}{2}} I_0(\alpha t) dt \quad (10)$$

is the Marcum Q-function, $I_p(\cdot)$ is the modified Bessel function of the first kind and order p , $g_m = \frac{1}{K} \mathbf{s}^H(u_0) \mathbf{s}(u_m)$, and $S \triangleq \frac{K}{\sigma_n^2} \sum_{t=0}^{M-1} |A(t)|^2$ may be interpreted as the total SNR integrated over the K antennas and the M snapshots.

2) Stochastic Signal Model (or Unconditional Model Assumption – UMA)

$$P_m = \frac{1}{(1 + q_m)^{2M-1}} \sum_{t=0}^{M-1} \binom{2M-1}{t} q_m^t \quad (11)$$

where

$$q_m = \frac{1 + \sqrt{1 + \frac{4\sigma_n^2(\sigma_n^2 + \sigma_s^2 K)}{\sigma_s^4 K^2 (1 - |g_m|^2)}}}{-1 + \sqrt{1 + \frac{4\sigma_n^2(\sigma_n^2 + \sigma_s^2 K)}{\sigma_s^4 K^2 (1 - |g_m|^2)}}} \quad (12)$$

where $\sigma_s^2 = E\{|A(t)|^2\}$ is the signal power.

The expressions in (9) and (11) are no longer valid if $N > 1$. They will be generalized for the multi-carrier case in the next two sections both for the deterministic and the stochastic signals model.

IV. EVALUATION OF THE PAIRWISE ERROR PROBABILITIES UNDER CMA

A. Theoretical derivation

In this Section, we derive the expression for the pairwise error probabilities under deterministic signal model, or Conditional Model Assumption.

The pairwise error probability in (6) can be written as

$$P_m = \Pr\{[V(u_m) > V(u_0)]\} = \Pr\{[V < 0]\} = \int_{-\infty}^0 p_V(V) dV \quad (13)$$

being $p_V(V)$ the pdf of the random variable $V = V(u_0) - V(u_m)$.

As it is apparent from (13), we need to evaluate the cumulative distribution function (CDF) of V in 0, i.e. $F_V(0)$. To this end, V can be rewritten as

$$V = V(u_0) - V(u_m) = \sum_{l=0}^{N-1} \sum_{t=0}^{M_l-1} |\mathbf{x}_l^H(t) \mathbf{P}_l \mathbf{x}_l(t)|^2 \quad (14)$$

where

$$\mathbf{P}_l = \mathbf{s}_l(u_0) \mathbf{s}_l^H(u_0) - \mathbf{s}_l(u_m) \mathbf{s}_l^H(u_m) \quad (l = 0, \dots, N-1) \quad (15)$$

is a rank-2 $K \times K$ Hermitian matrix.

By arranging the available snapshots in the $KL \times 1$ vector $\mathbf{x} = \frac{1}{\sigma_n} [\mathbf{x}_0^H(0) \dots \mathbf{x}_0^H(M_0-1) \mathbf{x}_1^H(0) \dots \mathbf{x}_{N-1}^H(M_{N-1}-1)]^H$ and by defining the corresponding $KL \times KL$ block diagonal matrix

$$\mathbf{P} = \sigma_n^2 \begin{bmatrix} \mathbf{I}_{M_0} \otimes \mathbf{P}_0 & \dots & \mathbf{0} \\ \vdots & \ddots & \vdots \\ \mathbf{0} & \dots & \mathbf{I}_{M_{N-1}} \otimes \mathbf{P}_{N-1} \end{bmatrix}, \text{ we can further simplify (14) as}$$

$$V = \mathbf{x}^H \mathbf{P} \mathbf{x} \quad (16)$$

By definition, the rank of \mathbf{P} is equal to $2L$. Specifically, it exhibits at most N pairs of distinct non-zero eigenvalues of equal magnitude but opposite sign. In the following, we assume that there are exactly N pairs of distinct eigenvalues, each with multiplicity M_l ($l = 0 \dots N-1$). In other words we suppose that different carrier frequencies selected from the considered set yield distinct pairs of eigenvalues. Notice that this hypothesis is mild and easily verified in practical cases. In fact, one can easily evaluate the non-zero eigenvalues of \mathbf{P} by using Theorem 18.1.1 in [34], thus obtaining

$$\begin{aligned} \gamma_l &= K \sigma_n^2 \sqrt{1 - |g_{m,l}|^2} \\ \gamma_{l+N} &= -K \sigma_n^2 \sqrt{1 - |g_{m,l}|^2} \end{aligned} \quad (17)$$

$$(l = 0, \dots, N-1)$$

where $g_{m,l} = \frac{1}{K} \mathbf{s}_l^H(u_0) \mathbf{s}_l(u_m)$ and we set $M_l = M_{l+N}$.

Let $\mathbf{P} = \mathbf{Q} \mathbf{\Lambda} \mathbf{Q}^H$ denote the eigenvalue decomposition of \mathbf{P} , we can assume that $\mathbf{\Lambda}$ is organized so that $\mathbf{\Lambda} = \begin{bmatrix} \bar{\mathbf{\Lambda}} & \mathbf{0}_{2L \times (KL-2L)} \\ \mathbf{0}_{(KL-2L) \times 2L} & \mathbf{0}_{(KL-2L) \times (KL-2L)} \end{bmatrix}$, where $\bar{\mathbf{\Lambda}}$ is a $2L \times 2L$ block with the non-zero eigenvalues on its main diagonal.

Equation (16) can be reworked as

$$V = (\mathbf{Q}^H \mathbf{x})^H \mathbf{\Lambda} \mathbf{Q}^H \mathbf{x} = \bar{\mathbf{x}}^H \bar{\mathbf{\Lambda}} \bar{\mathbf{x}} \quad (18)$$

where $\bar{\mathbf{x}} = \mathbf{S}^H (\mathbf{Q}^H \mathbf{x})$, $\mathbf{S} = [\mathbf{I}_{2L} \ ; \ \mathbf{0}_{2L \times (KL-2L)}]^H$.

Under the deterministic signal model, or CMA, \mathbf{x} is a complex Gaussian random vector, i.e. $\mathbf{x} \sim \mathcal{CN}(\mathbf{q}, \mathbf{I}_{KL})$ with mean vector

$$\mathbf{q} = \frac{1}{\sigma_n} [A_0^*(0) \mathbf{s}_0^H(u_0) \dots A_{N-1}^*(M_{N-1}-1) \mathbf{s}_{N-1}^H(u_0)]^H \quad (19)$$

Consequently, $\bar{\mathbf{x}} \sim \mathcal{CN}(\bar{\mathbf{q}}, \mathbf{I}_{2L})$, with $\bar{\mathbf{q}} = \mathbf{S}^H (\mathbf{Q}^H \mathbf{q})$, and (19) is usefully rewritten as

$$V = (\bar{\mathbf{h}} + \bar{\mathbf{q}})^H \bar{\mathbf{\Lambda}} (\bar{\mathbf{h}} + \bar{\mathbf{q}}) \quad (20)$$

where $\bar{\mathbf{h}}$ is a white zero-mean circularly symmetric complex Gaussian vector, i.e. $\bar{\mathbf{h}} \sim \mathcal{CN}(\mathbf{0}, \mathbf{I}_{2L})$.

Using the expression in (20) for the variable V , we can now exploit the approach in [30] to derive an approximation of the sought pairwise error probability. Specifically, the CDF of V can be written as

$$F_V(y) = \int_{-\infty}^{\infty} p(\bar{\mathbf{h}}) u(y - (\bar{\mathbf{h}} + \bar{\mathbf{q}})^H \bar{\mathbf{\Lambda}} (\bar{\mathbf{h}} + \bar{\mathbf{q}})) d\bar{\mathbf{h}} \quad (21)$$

where $p(\bar{\mathbf{h}})$ is the pdf of $\bar{\mathbf{h}}$ and $u(x)$ is the unit step function. Resorting to the Fourier transform representation or the unit step function

$$u(x) = \frac{1}{2\pi} \int_{-\infty}^{\infty} \frac{e^{x(j\omega+\beta)}}{j\omega+\beta} d\omega \quad \text{for any } \beta > 0 \quad (22)$$

one can write $F_V(y)$ as

$$F_V(y) = \frac{1}{2\pi^{2L+1}} \cdot \iint_{-\infty}^{\infty} e^{-\left(\|\bar{\mathbf{h}}\|^2 + (\bar{\mathbf{h}} + \bar{\mathbf{q}})^H (j\omega + \beta) \bar{\mathbf{\Lambda}} (\bar{\mathbf{h}} + \bar{\mathbf{q}})\right)} d\bar{\mathbf{h}} \frac{e^{y(j\omega+\beta)}}{j\omega+\beta} d\omega \quad (23)$$

that, solving the inner integral, yields

$$P_m = F_V(0) = \frac{1}{2\pi} \int_{-\infty}^{\infty} \frac{\exp\left\{-\bar{\mathbf{q}}^H \left(\mathbf{I}_{2L} + \frac{1}{(j\omega + \beta)\bar{\Lambda}^{-1}}\right)^{-1} \bar{\mathbf{q}}\right\}}{\det(\mathbf{I}_{2L} + (j\omega + \beta)\bar{\Lambda}) (j\omega + \beta)} d\omega \quad (24)$$

A closed form solution for the 1-D integral in (24) cannot be obtained [32]. Therefore, as in [30], we resort to the *Saddle Point (SP) technique* [33], which is a well-known method for approximating integrals. To this end, we write (24) as

$$F_V(0) = \frac{1}{2\pi} \int_{-\infty}^{\infty} e^{f(\omega)} d\omega \quad (25)$$

with

$$f(\omega) = -\ln(j\omega + \beta) - \sum_{k=0}^{2N-1} M_k \ln[1 + (j\omega + \beta)\gamma_k] - \sum_{k=0}^{2N-1} S_k \left(1 - \frac{1}{1 + (j\omega + \beta)\gamma_k}\right) \quad (26)$$

where $S_k = \sum_{j \in I(k)} |\bar{q}_j|^2$, and $I(k)$ containing the indices of the vector $\bar{\mathbf{q}}$ entries corresponding to the k -th eigenvalue ($|I(k)| = M_k$).

To apply the SP technique, we approximate $f(\omega)$ using a second order Taylor expansion around ω_0 , where $\omega_0 = j(\beta + p_0)$ is the solution of

$$f'(\omega) = -\sum_{k=0}^{2N-1} S_k \left[\frac{j\gamma_k}{(1 + (j\omega + \beta)\gamma_k)^2} \right] - \frac{j}{(j\omega + \beta)} - \sum_{k=0}^{2N-1} M_k \left[\frac{j\gamma_k}{1 + (j\omega + \beta)\gamma_k} \right] = 0 \quad (27)$$

with $p_0 \in (-\mu_{MAX}, 0)$, and $\mu_{MAX} = 1/\gamma_{MAX}$ being $\gamma_{MAX} = \max\{\gamma_k, k = 0, \dots, N-1\}$. Consequently, the integral in (25) can be approximated as

$$F_V(0) \approx \frac{1}{2\pi} e^{f(\omega_0)} \sqrt{\frac{2\pi}{|f''(\omega_0)|}} \quad (28)$$

By expliciting $f(\omega_0)$ and $f''(\omega_0)$, after some standard algebra, we eventually obtain

$$P_m = F_V(0) \approx \frac{|p_0|}{\sqrt{2\pi}} \exp\left\{-\sum_{k=0}^{2N-1} M_k \ln(1 - \gamma_k p_0) - \frac{S_k \gamma_k p_0}{1 - \gamma_k p_0}\right\} \times \left| -\frac{1}{p_0^2} - \sum_{k=0}^{2N-1} \frac{\gamma_k^2 M_k}{(1 - \gamma_k p_0)^2} + \frac{2\gamma_k^2 S_k}{(1 - \gamma_k p_0)^3} \right|^{-1/2} \quad (29)$$

B. Simulation Results

We first verify the accuracy of the approximation in (29), by comparing it with its exact expression when available (i.e. for $N = 1$, see (9)).

In Fig. 2(a) we report the normalized theoretical MF beampattern $V_{theo}(u)$ in (7) for a three-element array with element position $d = [0 \ 2 \ 6.8] \lambda_1$, where λ_1 is the wavelength of the exploited frequency channel and the DoA of the signal source is $u_0 = 0$. As it is apparent we considered a quite challenging array layout that is likely to yield outlier DoA estimates being the number of elements quite small and their spacing well above the employed wavelength. Consequently, a generally high sidelobe level is observed.

The most relevant sidelobe leading to outliers when the SNR decreases is indeed the highest sidelobe (indicated by the red arrow in Fig. 2 (a)). It represents the selected sidelobe where the pairwise error probability P_m is evaluated in Fig. 2 (b) for different SNR values, versus the number M of snapshots collected. Specifically we refer to the SNR at the single antenna element, for the single snapshot, i.e. $\text{SNR} \triangleq \frac{1}{\sigma_n^2 M} \sum_{t=0}^{M-1} |A(t)|^2$.

Fig. 2 (b) shows that the P_m expression derived in (29) is able to approximate the pairwise error probability in (9), even for very low values, e.g. $P_m = 10^{-20}$.

In Fig. 3 we compare the normalized theoretical MF beampattern $V_{theo}(u)$ of Fig. 2 (a) with that obtained exploiting three different frequency channels ($N = 3$) with wavelengths λ_1 , $\lambda_2 = 0.76 \lambda_1$, and $\lambda_3 = 0.57 \lambda_1$, respectively. It is expected that the asymptotic DoA estimation accuracy could benefit from the joint exploitation of signals with higher carrier frequencies. However we observe that the additional frequency channels considered in this case study are more critical in term of outliers when separately employed with the same array of Fig. 2.

Nevertheless, Fig. 3 shows that the sidelobe level is fruitfully reduced if the frequency diversity is exploited. Accordingly, we expect the probability of outlier to be lower since a higher noise level would be required for the sidelobes to exceed the main lobe peak. Clearly, the lower the probability of outlier, the higher the number of Monte Carlo simulation trials necessary to estimate such a rare event, i.e. the availability of a closed-form reliable expression to predict the estimator performance becomes more and more relevant.

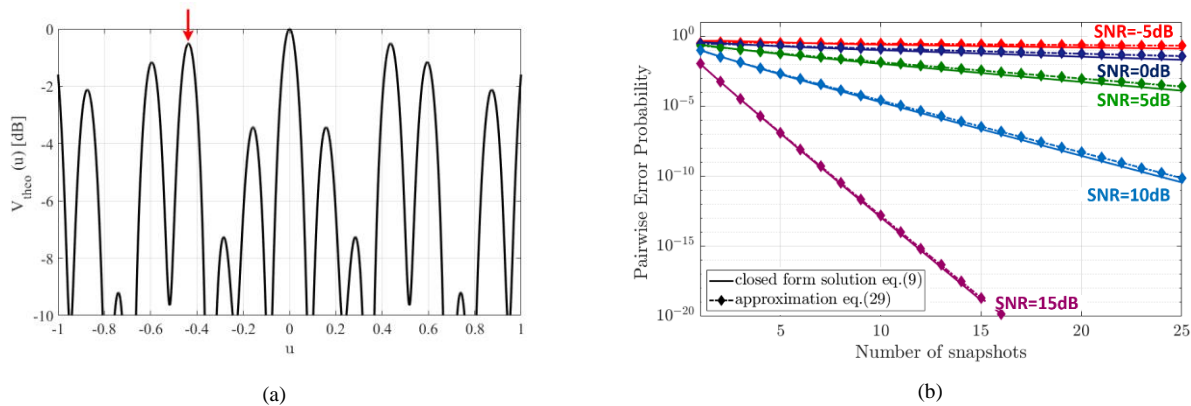


Fig. 2 – Results for a single frequency case ($N = 1$) with three-element array $d = [0 \ 2 \ 6.8] \lambda_1$
 (a) Theoretical MF beampattern $V_{theo}(u)$;
 (b) Pairwise error probability for a selected sidelobe for different values of SNR versus the number of snapshots.

To check the accuracy of the union bound approximation for the probability of outlier, we performed Monte Carlo (MC) simulations for different configurations. In all cases, the number of MC trials was 10^6 , whereas this number was increased to $5 \cdot 10^7$ when the probability of outlier P_o was expected to be below 10^{-4} . The outcome of the DoA estimation stage is labelled as “outlier” if it falls outside the mainlobe of the theoretical MF beampattern $V_{theo}(u)$. Each outlier is associated with the closest sidelobe peak, according to a minimum distance criterion. We compare the results of the MC simulations with the probability of outlier evaluated as in (6) by using the result in (29) at each sidelobe peak. Although the positions of these peaks are usually not available in closed form, they can be readily calculated by some numerical methods.

In Fig. 4, we compare the probability of outlier P_o with the results of MC simulations (dots) for different SNR. The SNR_{*l*} at the *l*-th frequency channel is defined as $SNR_l \triangleq \frac{1}{\sigma_n^2 M_l} \sum_{t=0}^{M_l-1} |A_l(t)|^2$, where the same SNR level is assumed for the employed frequency channels.

The results are reported for the case studies in Table I. For cases A and B also the P_o obtained with the exact expression in (9) is reported, in solid black line, for comparison.

Observing Fig. 4 the following considerations are in order:

- the expression in (29) effectively approximates the closed form solution, when available.
- The union bound approximation is quite robust for high SNR whereas it overestimates the probability of outlier at very low SNR values, where the simplified hypotheses behind (6) are no longer verified. However this is not expected to be an issue since those values are likely to correspond to the no information region.
- As expected, the higher the total number *L* of snapshots (collected either in time or in frequency domains) the better the performance.
- Keeping constant the total number of snapshots, better results can be obtained if they are collected at different

frequency channels (compare the green and light blue lines), revealing that the frequency diversity is essential besides the expected increase in integrated SNR. Basically, case B yields a gain of approximately 5 dB for P_o values below 10^{-2} whereas case C provides an additional gain of 7 dB.

- The last consideration is confirmed comparing case B and case E (see the green and magenta lines). In fact, even if two out of three frequency channels provide a lower SNR, their exploitation still allows to significantly reduce the probability of outlier with respect to the situation using $M = 3$ snapshots from the frequency channel with the highest SNR. This is due to the improvement arising in term of sidelobes level in the resulting multi-frequency likelihood function.
- When exploiting three snapshots from three frequency channels, the improvement is significant with respect to $L = 1$, since case D benefits from both the resulting SNR integration and the diversity of information conveyed by the multi-frequency approach.

V. EVALUATION OF THE PAIRWISE ERROR PROBABILITIES UNDER UMA

A. Theoretical derivation

In this Section, we derive the expression for the pairwise error probabilities under stochastic signal model, or UMA.

By proceeding as in Section IV, we obtain the same expression as in (16). However, under UMA, vector \mathbf{x} is a set of statistically independent *K*-dimensional complex Gaussian random variables, with zero-mean vector and covariance matrix \mathbf{R} , i.e. $\mathbf{x} \sim \mathcal{CN}(\mathbf{0}, \mathbf{R})$, where $\mathbf{R} = \begin{bmatrix} \mathbf{I}_{M_0} \otimes \mathbf{R}_0 & \cdots & \mathbf{0} \\ \vdots & \ddots & \vdots \\ \mathbf{0} & \cdots & \mathbf{I}_{M_{N-1}} \otimes \mathbf{R}_{N-1} \end{bmatrix}$ and the $K \times K$ blocks on

the main diagonal are given by $\mathbf{R}_l = \frac{\sigma_{s,l}^2}{\sigma_n^2} \mathbf{s}_l(u_0) \mathbf{s}_l(u_0)^H + \mathbf{I}_K$ ($l = 0, \dots, N-1$), with $\sigma_{s,l}^2 = E\{|A_l(t)|^2\}$ being the power of the l -th signal. Thus, V in (16) is a complex central quadratic form.

Without loss of generality, we can consider the central quadratic form in the variable \mathbf{x}_w which is the whitened version of \mathbf{x}

$$\begin{aligned} \mathbf{x}_w &= (\mathbf{R}^{-1/2})^H \mathbf{x} \\ \mathbf{P}_w &= (\mathbf{R}^{1/2})^H \mathbf{P} (\mathbf{R}^{1/2}) \end{aligned} \quad (30)$$

The rank of matrix \mathbf{P}_w is equal to $2L$ and it has at most N pairs of distinct non-zero eigenvalues.

As in Section IV.A, we suppose that there are exactly N pairs of distinct eigenvalues, each with multiplicity M_l ($l = 0, \dots, N-1$), given by

$$\begin{aligned} \gamma_l &= -\frac{K^2 \sigma_{s,l}^2 (1 - |g_{m,l}|^2)}{2} \left[-1 - \sqrt{1 + \frac{4\sigma_n^2 (\sigma_n^2 + \sigma_{s,l}^2 K)}{\sigma_{s,l}^4 K^2 (1 - |g_{m,l}|^2)}} \right] \\ \gamma_{l+N} &= -\frac{K^2 \sigma_{s,l}^2 (1 - |g_{m,l}|^2)}{2} \left[-1 + \sqrt{1 + \frac{4\sigma_n^2 (\sigma_n^2 + \sigma_{s,l}^2 K)}{\sigma_{s,l}^4 K^2 (1 - |g_{m,l}|^2)}} \right] \end{aligned} \quad (31)$$

$(l = 0, \dots, N-1)$

Denoting by $\mathbf{P}_w = \mathbf{Q}_w \mathbf{\Lambda}_w \mathbf{Q}_w^H$ the eigenvalue decomposition of \mathbf{P}_w , we can assume that $\mathbf{\Lambda}_w$ is organized so that $\mathbf{\Lambda}_w = \begin{bmatrix} \bar{\mathbf{\Lambda}}_w & \mathbf{0}_{2L \times (KL-2L)} \\ \mathbf{0}_{(KL-2L) \times 2L} & \mathbf{0}_{(KL-2L) \times (KL-2L)} \end{bmatrix}$ where $\bar{\mathbf{\Lambda}}_w$ is a $2L \times 2L$ diagonal matrix containing the non-zero eigenvalues on its main diagonal.

Therefore, under UMA, the CDF of V can be written as

$$F_V(y) = \frac{1}{2\pi} \int_{-\infty}^{\infty} \frac{e^{y(j\omega + \beta)}}{\det(\mathbf{I}_{2L} + (j\omega + \beta)\bar{\mathbf{\Lambda}}) (j\omega + \beta)} d\omega \quad (32)$$

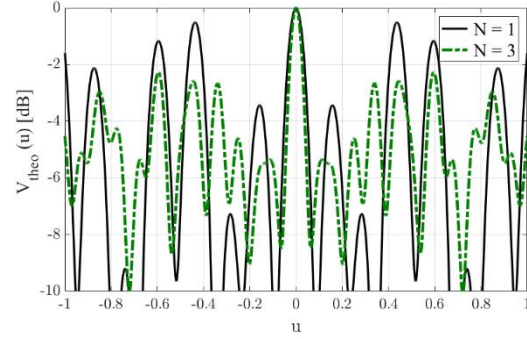


Fig. 3 – Theoretical MF beampattern $V_{theo}(u)$ for three-element array $d = [0 \ 2 \ 6.8] \lambda_1$, exploiting one or three frequency channels

The integral in (32) has a closed form solution that can be derived as in [30]. First, resorting to the partial fraction expansion, we can write

$$\frac{1}{\det(\mathbf{I}_{2L} + (j\omega + \beta)\bar{\mathbf{\Lambda}}) (j\omega + \beta)} = \sum_{k=0}^{2N-1} \sum_{t=0}^{M_k-1} \frac{\alpha_{k,t}}{(1 + \gamma_k(j\omega + \beta))^{t+1}} + \frac{1}{(j\omega + \beta)} \quad (33)$$

where the coefficients $\alpha_{k,t}$ are given by

$$\begin{aligned} \alpha_{k,t} &= \frac{1}{\Gamma(M_k - t)} \left[\prod_{n=0}^{2N-1} \mu_n^{M_n} \right] y_k^{(M_k-t-1)}(s) \Big|_{s=-\mu_k} \\ &(k = 0, \dots, 2N-1, \quad t = 0, \dots, M_k-1) \end{aligned} \quad (34)$$

with $y_k^{(M_k-t-1)}(s)$ the $(M_k - t - 1)$ -th derivative of $y_k(s)$, defined as

TABLE I
CASE STUDIES A-E

	Number of array elements (K)	Number of carriers (N)	Number of snapshots (M)	Array	Wavelengths	SNR
case A	3	1	1	$d = [0 \ 2 \ 6.8] \lambda_1$	λ_1	–
case B	3	1	3	$d = [0 \ 2 \ 6.8] \lambda_1$	λ_1	–
case C	3	3	1	$d = [0 \ 2 \ 6.8] \lambda_1$	$\lambda_1, \lambda_2 = 0.76 \lambda_1, \lambda_3 = 0.57 \lambda_1$	$\text{SNR}_1 = \text{SNR}_2 = \text{SNR}_3$
case D	3	3	3	$d = [0 \ 2 \ 6.8] \lambda_1$	$\lambda_1, \lambda_2 = 0.76 \lambda_1, \lambda_3 = 0.57 \lambda_1$	$\text{SNR}_1 = \text{SNR}_2 = \text{SNR}_3$
case E	3	3	1	$d = [0 \ 2 \ 6.8] \lambda_1$	$\lambda_1, \lambda_2 = 0.76 \lambda_1, \lambda_3 = 0.57 \lambda_1$	$\text{SNR}_2 = \text{SNR}_3 = \text{SNR}_1 - 3\text{dB}$

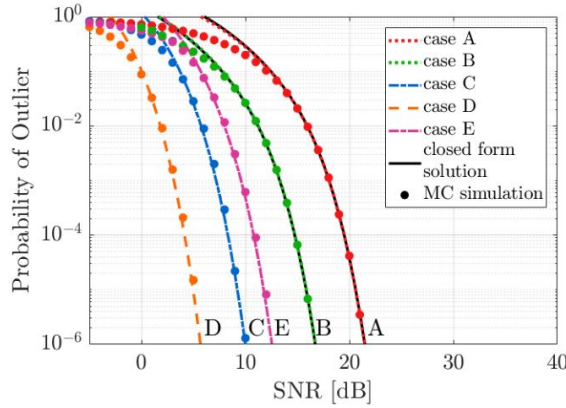


Fig. 4 – Probability of outlier under CMA for a three-element array $d = [0 \ 2 \ 6.8] \lambda_1$ and :
 - **case A**: one snapshot ($M = 1$) from one frequency channel ($N = 1$)
 - **case B**: three snapshots ($M = 3$) from one frequency channel ($N = 1$)
 - **case C**: one snapshot ($M = 1$) from each of the three frequency channels ($N = 3$) with wavelengths $\lambda_1, \lambda_2, \lambda_3$
 - **case D**: three snapshots ($M = 3$) from each of the three frequency channels ($N = 3$) with wavelengths $\lambda_1, \lambda_2, \lambda_3$
 - **case E**: one snapshot ($M = 1$) from each of the three frequency channels ($N = 3$) with wavelengths $\lambda_1, \lambda_2, \lambda_3$, with $\text{SNR}_2 = \text{SNR}_3 = \text{SNR}_1 - 3\text{dB}$

$$y_k(s) = \prod_{\substack{n=0 \\ n \neq k}}^{2N} (\mu_n + s)^{-M_n} \quad (35)$$

with $\mu_n = \frac{1}{\gamma_n}$ ($n = 0, \dots, 2N - 1$), $\mu_{2N} = 0$ and $M_{2N} = 1$.

Now, using the expression in (33), we can split the integral in (32) in two parts and evaluate them separately. Eventually, after some calculations, we obtain a closed form solution

$$P_m = F_V(0) = \frac{1}{2} \left[1 + \sum_{k=0}^{2N-1} \text{sign}(\gamma_k) \cdot \alpha_{k,0} \right] \quad (36)$$

One can evaluate the coefficient $y_k^{(M_n-1)}$ in $\alpha_{k,0}$ differentiating the logarithm of $y_k(s)$, i.e. $\frac{d}{ds} \log(y_k(s)) = \frac{1}{y_k(s)} y_k^{(1)}(s)$, that yields

$$y_k^{(1)}(s) = -y_k(s) \sum_{\substack{n=0 \\ n \neq k}}^{2N} M_n (\mu_n + s)^{-1} \quad (37)$$

Subsequently, Leibniz's rule for differentiation of products may be applied. Thus, the required coefficients can be evaluated using the following recursion formula

$$y_k^{(p)}(s) \Big|_{s=-\mu_k} = \frac{d^{p-1}}{ds^{p-1}} y_k^{(1)}(s) \Big|_{s=-\mu_k} = \sum_{r=0}^{p-1} \sum_{\substack{n=0 \\ n \neq k}}^{2N} M_n \binom{p-1}{r} \frac{(-1)^{p-r} \Gamma(p-r)}{(\mu_n - \mu_k)^{p-r}} y_k^{(r)}(s) \Big|_{s=-\mu_k} \quad (38)$$

$(p \geq 1)$

$$y_k^{(0)}(s) \Big|_{s=-\mu_k} = y_k(-\mu_k) = \prod_{\substack{n=0 \\ n \neq k}}^{2N} (\mu_n - \mu_k)^{-M_n}$$

Equation (36), with coefficients obtained using (34) and (38), provides a closed form expression of the pairwise error probability under UMA for the m -th sidelobe peak.

In particular, for the single-frequency case, namely when $N = 1$ and $M \geq 1$, it coincides with the solution in (11), being $q_m = \left| \frac{\gamma_0}{\gamma_1} \right|$ the ratio between the absolute values of the two eigenvalues.

In the dual special case, namely when $M = 1$ and $N \geq 1$, with the assumptions made on the distinct eigenvalues, we have $M_k = 1$ ($k = 0, \dots, 2N$). Consequently, we can write the residues $\alpha_{k,0}$ as

$$\alpha_{k,0} = \frac{\prod_{n=0}^{2N-1} \mu_n}{\prod_{\substack{n=0 \\ n \neq k}}^{2N} (\mu_n - \mu_k)} \quad (39)$$

$(k = 0, \dots, 2N - 1)$

B. Simulation Results

To verify the accuracy of the expression in (36), Fig. 5 compares the results of MC simulations with the probability of outlier evaluated using (6) and P_m obtained from (36) under stochastic signal model.

The results are reported versus SNR, being in this case $\text{SNR}_l \triangleq \frac{\sigma_{s,l}^2}{\sigma_n^2}$. The same methodology is adopted as in Section IV.B, and the same three-element array layout $d = [0 \ 2 \ 6.8] \lambda_1$ is employed together with some representative case studies, namely those B,C and D.

Observing Fig. 5, some of the considerations made with reference to Fig. 4 under CMA can be confirmed also under UMA. In addition, we notice that:

- when very few snapshots are available (collected either in time or in frequency), the union bound approximation slightly overestimates the probability of outlier also for high SNR values (see cases B and C); similar results were obtained also in [19] for the single-carrier case.

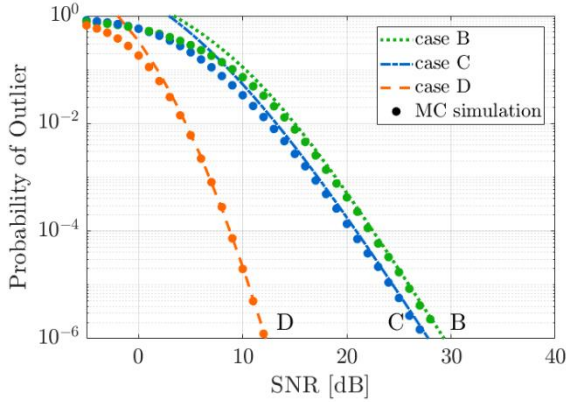


Fig. 5 – Probability of outlier under UMA for a three elements array $d = [0 \ 2 \ 6.8] \lambda_1$ and

- case B: three snapshots ($M = 3$) from one frequency channel ($N = 1$)
- case C: one snapshot ($M = 1$) from each of the three frequency channels ($N = 3$) with wavelengths $\lambda_1, \lambda_2, \lambda_3$
- case D: three snapshots ($M = 3$) from each of the three frequency channels ($N = 3$) with wavelengths $\lambda_1, \lambda_2, \lambda_3$

- Increasing the number of snapshots, the union bound approximation seems quite robust for high SNR, whereas it still is not very tight for very low SNR values (see case D). However, as aforementioned, those values are likely to correspond to the no information region.
- Compared with Fig. 4, a higher probability of outlier can be obtained under UMA for the same case study. The benefits provided by frequency diversity become smaller and smaller when few snapshots are available. In contrast, the gain resulting from the availability of multi-frequency observations becomes quite evident increasing the number of snapshots collected at each carrier frequency, especially for low values of the probability of outlier.

VI. SIMULATION RESULTS : MSE APPROXIMATION

So far we have investigated the robustness of the expressions characterizing the pairwise error probability under CMA and under UMA in the multi-carrier case with reference to the the probability of outlier.

In this section, the identified expressions are used to provide an accurate characterization of the MF ML DoA estimator performance for a multi-channel receiver operating in the threshold region.

To this end, we resort to the approximate formula in (8) where

- P_m is given by (29) or (36) depending on the signal model, namely CMA or UMA;
- the CRB can be easily evaluated starting from the general expression of the Fisher information matrix $I(\theta)$ for the problem under consideration [35]

$$I(\theta)^{(p,k)} = \text{Tr} \left(\frac{\partial \Gamma(\zeta)}{\partial \zeta^{(p)}} \Gamma^{-1}(\zeta) \frac{\partial \Gamma(\zeta)}{\partial \zeta^{(k)}} \Gamma^{-1}(\zeta) \right) + 2 \text{Re} \left(\frac{\partial \mathbf{m}^H(\zeta)}{\partial \zeta^{(p)}} \Gamma^{-1}(\zeta) \frac{\partial \mathbf{m}(\zeta)}{\partial \zeta^{(k)}} \right) \quad (40)$$

where $\Gamma(\zeta)$ and $\mathbf{m}(\zeta)$ are the covariance matrix and the mean vector of the received signal \mathbf{x} and depend on a set of unknown parameters ζ , being ζ a W -dimensional vector, so that $p, k = 0, \dots, W - 1$.

The application of (40) to the DoA estimation problem of interest herein yields two different expressions for the CRB, relative to the deterministic and stochastic signal models.

1) Deterministic Signal Model (or CMA)

According to the definitions in Sections IV, we would have $\zeta = [u_0 \ A_0(0) \dots A_0(M_0 - 1) \dots A_{N-1}(M_{N-1} - 1)]$, namely $W = L + 1$, $\mathbf{m}(\zeta) = \mathbf{q}$, being \mathbf{q} defined in (19) and $\Gamma(\zeta) = \Gamma = \mathbf{I}_{KL}$. Therefore, after some algebra, the following expression is obtained

$$\text{CRB}_{\text{CMA}}(u_0) = \left[8\pi^2 \sum_{k=0}^{K-1} \left(d_k - \frac{1}{K} \sum_{p=0}^{K-1} d_p \right)^2 \sum_{l=0}^{N-1} \frac{M_l \text{SNR}_l}{\lambda_l^2} \right]^{-1} \quad (41)$$

2) Stochastic Signal Model (or UMA)

According to the definitions in Sections V, the set of unknown parameters would be reduced to a scalar $\zeta = u_0$, namely $W = 1$, while $\mathbf{m}(\zeta) = \mathbf{0}$ and $\Gamma(\zeta) = \mathbf{R}$. Therefore, after some algebra, the following expression is obtained

$$\text{CBR}_{\text{UMA}}(u_0) = \left[8\pi^2 \sum_{k=0}^{K-1} \left(d_k - \frac{1}{K} \sum_{p=0}^{K-1} d_p \right)^2 \sum_{l=0}^{N-1} \frac{M_l \text{SNR}_l^2 K}{\lambda_l^2 (1 + K \text{SNR}_l)} \right]^{-1} \quad (42)$$

In both cases, the array layout affects the performance via the term $G = \sum_{k=0}^{K-1} \left(d_k - \frac{1}{K} \sum_{p=0}^{K-1} d_p \right)^2$ that basically measures the mean square distance of the array elements from a baricenter. Larger arrays (in the sense that the factor G is higher) yield better asymptotic performance. However, a given layout yields a different impact when employed at different carrier frequencies and this impact is related to the SNR available at each frequency channel.

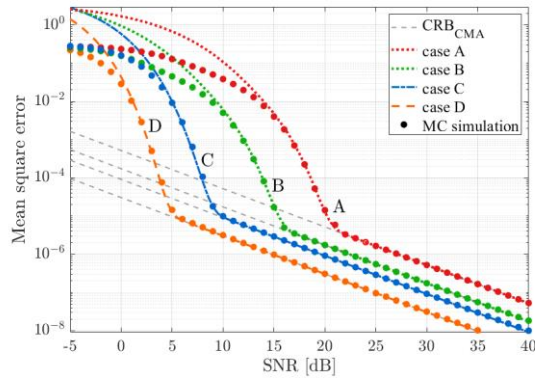


Fig. 6 – MSE approximation under CMA for a three-element array with elements positions $d = [0 \ 2 \ 6.8] \lambda_1$ and:
 - case A: one snapshot ($M = 1$) from one frequency channel ($N = 1$)
 - case B: three snapshots ($M = 3$) from one frequency channel ($N = 1$)
 - case C: one snapshot ($M = 1$) from each of the three frequency channels ($N = 3$) with wavelengths $\lambda_1, \lambda_2, \lambda_3$
 - case D: three snapshots ($M = 3$) from each of the three frequency channels ($N = 3$) with wavelengths $\lambda_1, \lambda_2, \lambda_3$

As expected, (42) tends to (41) for high SNR values.

In the following, aiming at demonstrating the reliability of the MSE approximation in (8) when using the expressions in (29), (36), (41) and (42), we compare the theoretical performance to the results of MC simulations. As in Section IV, the number of trials was set to 10^6 and it was increased to $5 \cdot 10^7$ for SNR values such that $P_o < 10^{-4}$.

In particular, Fig. 6 shows the comparison between the MSE approximation and the results of MC simulations (dots) versus the SNR under CMA for case studies A-D, defined in Section IV.B (see Table I). The corresponding CRB for each case is also reported in dashed gray.

The three operative regions are quite easily identified and, as expected, the CRB is not able to model the ML estimator

performance is the threshold region. In contrast, the MSE approximation considered in this paper is quite accurate in representing the performance of the estimator both in the threshold and the asymptotic region. In particular, this consideration applies both to the single-frequency cases A-B and to the multi-frequency situations C-D.

We observe that in the former situations, the results of [19] could have been fruitfully exploited. However the reported analysis demonstrates that the approximate expression in (29) for the pairwise error probability provides a reliable tool that can be exploited either when a single frequency channel is available and when a multi-carrier receiver is considered.

Remarkably, the approximate MSE can be successfully exploited to evaluate the lower limit SNR value that represents the boundary between the threshold region and the asymptotic region, namely the threshold SNR value. This value is heavily dependent on the probability of outlier (see Fig. 4): in each considered case, the MSE significantly deviates from the CRB curve when P_o gets above 10^{-5} . This could represent an interesting point of view when comparing different array layouts and frequency channels combinations.

For instance we report in Fig. 7 the results obtained using two different array layouts for a four-element array when $M_l = M = 1$ ($l = 0, \dots, N - 1$) snapshot is collected from each of the $N = 3$ frequency channels ($L = 3$). Specifically, we consider the case studies F,G and H in Table II.

Observing Fig. 7, we notice that the more effective configuration in the asymptotic region is not necessarily the best also in the threshold region. Moreover, keeping constant the array layout and the number of frequency channels (e.g. see cases G and H), the choice of the carrier frequencies has a non-negligible impact on the threshold value and this can be easily predicted using the proposed MSE approximation.

In Fig. 8 we compare the MSE approximation under UMA with the results of MC simulations versus the SNR for the aforementioned case studies C, D and H (see Table I and Table II).

TABLE II
CASE STUDIES F-I

	Number of array elements (K)	Number of carriers (N)	Number of snapshots (M)	Array	Wavelengths	SNR
case F	4	3	1	$d = [0 \ 3.8 \ 8.8 \ 15.5] \lambda_1$	$\lambda_1 \lambda_2 = 0.76 \lambda_1, \lambda_3 = 0.57 \lambda_1$	$\text{SNR}_1 = \text{SNR}_2 = \text{SNR}_3$
case G	4	3	1	$d = [0 \ 2 \ 6.8 \ 10] \lambda_1$	$\lambda_1 \lambda_2 = 0.76 \lambda_1, \lambda_3 = 0.57 \lambda_1$	$\text{SNR}_1 = \text{SNR}_2 = \text{SNR}_3$
case H	4	3	1	$d = [0 \ 2 \ 6.8 \ 10] \lambda_1$	$\lambda_1, \lambda_3 = 0.57 \lambda_1, \lambda_4 = 0.68 \lambda_1$	$\text{SNR}_1 = \text{SNR}_2 = \text{SNR}_4$
case I	4	4	1	$d = [0 \ 2 \ 6.8 \ 10] \lambda_1$	$\lambda_1, \lambda_2 = 0.76 \lambda_1, \lambda_3 = 0.57 \lambda_1, \lambda_4 = 0.68 \lambda_1$	$\text{SNR}_1 = \text{SNR}_2 = \text{SNR}_3 = \text{SNR}_4$

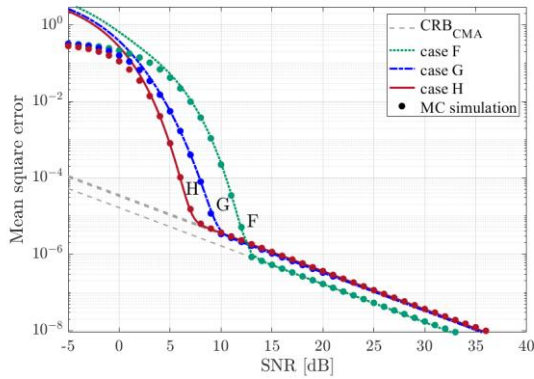


Fig. 7 –MSE approximation under CMA for four-element array with different elements positions and one snapshot ($M = 1$) from each of three frequency channels ($N = 3$):

- case F: $d = [0 \ 3.8 \ 8.8 \ 15.5] \lambda_1$ exploiting $\lambda_1, \lambda_2, \lambda_3$
- case G: $d = [0 \ 2 \ 6.8 \ 10] \lambda_1$ exploiting $\lambda_1, \lambda_3, \lambda_4$
- case H: $d = [0 \ 2 \ 6.8 \ 10] \lambda_1$ exploiting $\lambda_1, \lambda_2, \lambda_3$

Moreover, a new situation is also introduced, namely case I, exploiting the same three-element array as in C and D but with $M_l = M = 1$ ($l = 0, \dots, N - 1$) snapshot from each of the $N = 4$ frequency channels (see Table II for details).

The following considerations are in order:

- the three operative regions are still quite easily identified for all cases.
- When only three snapshots are collected (see cases C and H), the MSE approximation slightly overestimates the performance in the threshold region. This is due to the fact that the union bound approximation does not appear tight in that situation, see e.g. case C in Fig. 5.
- Compared to Fig. 6 and Fig. 7, a high MSE is obtained under UMA with respect to CMA for the same case studies (see cases C,D and H).
- The exploitation of one additional snapshot collected from a different frequency channel allows to decrease significantly the MSE (e.g. compare cases C and I) thus reducing the threshold SNR value.
- Since a larger array is used in case H, a better asymptotic performance is reached with respect to case I. This is no longer true when comparing performances in the threshold region. This behavior highlights that frequency diversity might be more useful than spatial diversity when few antenna elements are employed.
- Although cases D and H exhibit a very similar asymptotic performance, the threshold SNR value is quite different for the two configurations. This is expected since a three times higher number of snapshots is available in case D ($L = 9$).

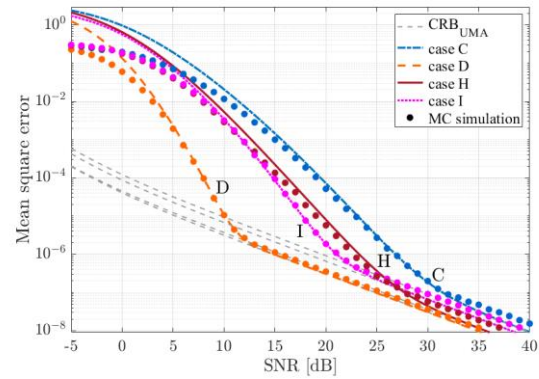


Fig. 8 – MSE approximation under UMA and:

- case C: three-element array with positions : $d = [0 \ 2 \ 6.8] \lambda_1$ and one snapshot ($M = 1$) from each of three frequency channels ($N = 3$) with wavelengths $\lambda_1, \lambda_2, \lambda_3$
- case D: three-element array with positions : $d = [0 \ 2 \ 6.8] \lambda_1$ and three snapshots ($M = 3$) from each of three frequency channels ($N = 3$) with wavelengths $\lambda_1, \lambda_2, \lambda_3$
- case H: four-element array with positions $d = [0 \ 2 \ 6.8 \ 10] \lambda_1$ and one snapshot ($M = 1$) from each of three frequency channels ($N = 3$) with wavelengths $\lambda_1, \lambda_2, \lambda_3$
- case I: three-element array with positions : $d = [0 \ 2 \ 6.8] \lambda_1$ and one snapshot ($M = 1$) from each of four frequency channels ($N = 4$) with wavelengths $\lambda_1, \lambda_2, \lambda_3, \lambda_4$

VII. CONCLUSIONS

Appropriate approximations to the MSE of a multi-frequency DoA ML estimator have been introduced in this paper to provide a reliable performance characterization in the threshold region. The reported analysis showed that the proposed MSE approximations are effectively able to model the performance of the estimator employing multiple observation possibly collected at different frequency channels both under CMA and under UMA.

The capability of predicting the threshold SNR value could be a powerful tool that can be used in order to optimize the receiving system design. For instance it can be exploited to identify a suitable array layout with the aim to control the insurgence of statistical ambiguities on target localization, especially in systems typically operating with low SNR levels and few antenna elements. Possible future research avenues could also concern the extension of the framework to different amplitude fluctuation models (such as Swerling [36],[37] or Weibull [38]) which are relevant in some radar applications.

REFERENCES

- [1] Krim H. and Viberg M., "Two decades of array signal processing research: the parametric approach," in *IEEE Signal Processing Magazine*, vol. 13, no. 4, pp. 67-94, 1996
- [2] Van Trees H. L., "Detection, Estimation, and Modulation Theory, Part IV, Optimum Array Processing," New York, NY, USA, Wiley, 2002
- [3] Schmidt R. O., "Multiple emitter location and signal parameter estimation," in *IEEE Transactions on Antennas and Propagation*, vol. AP-34, no. 3, pp. 276-280, Mar. 1986
- [4] Roy R. and Kailath T., "ESPRIT-estimation of signal parameters via rotational invariance techniques," in *IEEE Transactions on Acoustics, Speech and Signal Processing*, vol. 37, no. 7, pp. 984-995, Jul. 1989
- [5] Stoica P. and Nehorai A., "MUSIC, maximum likelihood, and Cramer-Rao bound," in *IEEE Transactions on Acoustics, Speech and Signal Processing*, vol. 37, pp. 720-741, May 1989
- [6] Stoica P. and Nehorai A., "Performance study of conditional and unconditional direction-of-arrival estimation," in *IEEE Transactions on Acoustics, Speech, and Signal Processing*, vol. 38, no. 10, pp. 1783-1795, Oct 1990
- [7] Ottersten B., Viberg M., Stoica P., and Nehorai A., "Exact and large sample maximum likelihood techniques for parameter estimation and detection in array processing," in *Radar Array Processing*, S. Haykin, J. Litva, and T. J. Shepherd, Eds. Berlin, Germany: Springer-Verlag, 1993, ch. 4, pp. 99-151
- [8] Gershman A. B., Stoica P., Pesavento M. and Larsson E. G., "Stochastic Cramer-Rao bound for direction estimation in unknown noise fields," in *IEE Proceedings - Radar, Sonar and Navigation*, vol. 149, no. 1, pp. 2-8, Feb 2002
- [9] Van Trees H. L., *Detection, estimation and modulation theory*, Part I, John Wiley and Sons Inc., 1968
- [10] Rife D. C. and Boorstyn R. R., "Single-tone parameter estimation from discrete-time observations," in *IEEE Transactions on Information Theory*, vol. 20, no. 5, pp. 591-598, Sep 1974
- [11] Stansfield R. G., "Statistical Theory of D.F. Fixing", *Journal of the Institution of Electrical Engineers - Part IIIA: Radiocommunication*, vol. 94, pp. 762-770, 1947
- [12] Torrieri D. J., "Statistical Theory of Passive Location Systems," in *IEEE Transactions on Aerospace and Electronic Systems*, vol. AES-20, no. 2, pp. 183-198, March 1984
- [13] Blachman N.M., "Position Determination from Radio Bearings," in *IEEE Transactions on Aerospace and Electronic Systems*, vol. AES-5, pp. 558-560, 1969
- [14] Howland P. E., "Target tracking using television-based bistatic radar," in *IEE Proceedings - Radar, Sonar and Navigation*, vol. 146, no. 3, pp. 166-174, Jun 1999
- [15] Colone F., Bongioanni C. and Lombardo P., "Multifrequency integration in FM radio-based passive bistatic radar. Part II: Direction of arrival estimation," in *IEEE Aerospace and Electronic Systems Magazine*, vol. 28, no. 4, pp. 40-47, April 2013
- [16] Filippini F., Martelli T., Colone F. and Cardinali R., "Target DoA estimation in passive radar using non-uniform linear arrays and multiple frequency channels," *2018 IEEE Radar Conference (RadarConf18)*, Oklahoma City, OK, 2018, pp. 1290-1295
- [17] Pasupathy S. and Alford W. J., "Range and Bearing Estimation in Passive Sonar," in *IEEE Transactions on Aerospace and Electronic Systems*, vol. AES-16, no. 2, pp. 244-249, March 1980
- [18] Van Trees H.L. and Bell K.L., *Bayesian Bounds for Parameter Estimation and Nonlinear Filtering/Tracking*, Wiley, New York (2007)
- [19] Athley F., "Threshold region performance of maximum likelihood direction of arrival estimators," in *IEEE Transactions on Signal Processing*, vol. 53, no. 4, pp. 1359-1373, Apr. 2005
- [20] Richmond C. D., "Mean-squared error and threshold SNR prediction of maximum-likelihood signal parameter estimation with estimated colored noise covariances," in *IEEE Transactions on Information Theory*, vol. 52, no. 5, pp. 2146-2164, May 2006
- [21] Abramovich Y. I. and Johnson B. A., "Threshold performance for conditional and unconditional direction of arrival estimation," *2012 Conference Record of the Forty Sixth Asilomar Conference on Signals, Systems and Computers (ASILOMAR)*, Pacific Grove, CA, 2012, pp. 5-12
- [22] Barankin E. W., "Locally best unbiased estimates," *Ann. Math. Stat.*, vol. 20, pp. 477-501, 1949
- [23] Ziv J. and Zakai M., "Some lower bounds on signal parameter estimation," in *IEEE Transactions on Information Theory*, vol. 15, no. 3, pp. 386-391, May 1969
- [24] Wang W. Q., "Frequency Diverse Array Antenna: New Opportunities," in *IEEE Antennas and Propagation Magazine*, vol. 57, no. 2, pp. 145-152, April 2015
- [25] Liu H., Zhou S., Su H. and Yu Y., "Detection performance of spatial-frequency diversity MIMO radar," in *IEEE Transactions on Aerospace and Electronic Systems*, vol. 50, no. 4, pp. 3137-3155, October 2014
- [26] Ulrich M. and Yang B., "Multi-carrier MIMO radar: A concept of sparse array for improved DOA estimation," *2016 IEEE Radar Conference (RadarConf)*, Philadelphia, PA, 2016, pp. 1-5
- [27] BouDaher E., Jia Y., Ahmad F. and Amin M. G., "Multi-Frequency Co-Prime Arrays for High-Resolution Direction-of-Arrival Estimation," in *IEEE Transactions on Signal Processing*, vol. 63, no. 14, pp. 3797-3808, July 2015
- [28] Skolnik M.I., "Resolution of angular ambiguities in radar array antennas with widely-spaced elements and grating lobes," in *IRE Transactions on Antennas and Propagation*, vol. AP-10, pp. 351-352, May 1962
- [29] Coutts S. D., "Passive localization of moving emitters using out-of-plane multipath," in *IEEE Transactions on Aerospace and Electronic Systems*, vol. 36, no. 2, pp. 584-595, April 2000.
- [30] Al-Naffouri T.Y., Moinuddin M., Ajeeb N., Hassibi B. and Moustakas A.L., "On the Distribution of Indefinite Quadratic Forms in Gaussian Random Variables," in *IEEE Transactions on Communications*, vol. 64, no. 1, pp. 153-165, Jan. 2016
- [31] Proakis J. G., "Digital Communications," 4th Edition, McGraw-Hill, New York, 2001
- [32] Simon M. K. and Alouini M.-S., "On the difference of two chi-square variates with application to outage probability computation," in *IEEE Transaction on Communications*, vol. 49, no.11, pp. 1946-1954, Nov. 2001
- [33] Bender C. M. and Orszag S. A., *Advanced Mathematical Methods for Scientists and Engineers*, New York, NY, USA, McGraw-Hill, 1978
- [34] Harville D. A., *Matrix Algebra From a Statistician's Perspective*, New York, NY, USA, Springer, 1997
- [35] Hung H. and Kaveh M., "On the statistical sufficiency of the coherently averaged covariance matrix for the estimation of the parameters of wideband sources," *ICASSP '87. IEEE International Conference on Acoustics, Speech, and Signal Processing*, 1987, pp. 33-36
- [36] Swerling P., "Probability of detection for fluctuating targets," in *IRE Transactions on Information Theory*, vol. 6, no. 2, pp. 269-308, April 1960
- [37] Swerling P., "Radar probability of detection for some additional fluctuating target cases," in *IEEE Transactions on Aerospace and Electronic Systems*, vol. 33, no. 2, pp. 698-709, April 1997
- [38] Cui G., De Maio A., Carotenuto V. and Pallotta L., "Performance prediction of the incoherent detector for a weibull fluctuating target," in *IEEE Transactions on Aerospace and Electronic Systems*, vol. 50, no. 3, pp. 2176-2184, July 2014



Francesca Filippini received both her B.Sc. and M.Sc. (*cum laude*) in Communication Engineering, from Sapienza University of Rome, Italy, in 2013 and 2016, respectively. From January to May 2016, she has been working on her Master Thesis as an intern of the Passive Radar and Anti-Jamming Techniques Department of Fraunhofer FHR, Germany.

She is currently working toward the Ph.D. degree in Radar and Remote Sensing at the Department of Information Engineering, Electronics and Telecommunications, Sapienza University of Rome. The central topic of her PhD research is the development of advanced signal processing techniques and methodologies for Passive Radar Systems.

She has been co-recipient of the 2018 Premium Award for Best Paper in IET Radar, Sonar & Navigation, she received the second best Student Paper Award at the 2018 IEEE Radar Conference in Oklahoma City, OK, USA and the Best Paper Award at the 2017 GTTI Workshop on Radar and Remote Sensing in Naples, Italy.

Since 2019, she is member of the Board of Governors of the IEEE Aerospace and Electronic System Society (AESS), where she is serving as Graduate Student Representative.



Fabiola Colone received the laurea degree (B.S.+M.S.) in Telecommunications Engineering and the Ph.D. degree in Remote Sensing from Sapienza University of Rome, Italy, in 2002 and 2006, respectively. She joined the DIET Dept. (formerly INFOCOM) of Sapienza University of Rome as a Research Associate in January 2006. From December 2006

to June 2007, she was a Visiting Scientist at the Electronic and Electrical Engineering Dept. of the University College London, London, U.K. She is currently an Associate Professor at the Faculty of Information Engineering, Informatics, and Statistics of Sapienza University of Rome.

The majority of Dr. Colone's research activity is devoted to radar systems and signal processing. She has been involved, with scientific responsibility roles, in research projects funded by the European Commission, the European Defence Agency, the Italian Space Agency, the Italian Ministry of Research, and the radar industry. Her research has been reported in over 120 publications in international technical journals, book chapters, and conference proceedings. Dr. Colone has been co-recipient of the 2018 Premium Award for Best Paper in IET Radar, Sonar & Navigation.

Since 2017 she is member of the Board of Governors of the IEEE Aerospace and Electronic System Society (AESS) in

which she is currently serving as Vice-President for Member Services, Chair of the AESS Professional Networking and Mentoring Program, and Editor in Chief for the IEEE AESS QEB Newsletters. She is IEEE Senior Member from 2017 and member of the IEEE AESS Radar System Panel from 2019. Dr. Colone is Associate Editor for the IEEE Transactions on Signal Processing and member of the Editorial Board of the Int. Journal of Electronics and Communications (Elsevier). She was in the organizing committee, as the Student Forum Co-Chair, of the IEEE 2008 Radar Conference (Rome, Italy), and she is currently in the organizing committee, as Special Sessions Co-Chair, of the IEEE 2020 Radar Conference (Florence, Italy). She served in the technical committee of many international conferences and she is frequently reviewer for a number of international technical journals.



Antonio De Maio (S'01–A'02–M'03–SM'07–F'13) was born in Sorrento, Italy, on June 20, 1974. He received the Dr.Eng. (Hons.) and Ph.D. degrees in information engineering from the University of Naples Federico II, Naples, Italy, in 1998 and 2002, respectively. From October to December 2004, he was a Visiting Researcher with the U.S. Air

Force Research Laboratory, Rome, NY, USA. From November to December 2007, he was a Visiting Researcher with the Chinese University of Hong Kong, Hong Kong. He is currently a Professor with the University of Naples Federico II. His research interest lies in the field of statistical signal processing, with emphasis on radar detection, optimization theory applied to radar signal processing, and multiple-access communications. He is the recipient of the 2010 IEEE Fred Nathanson Memorial Award as the young (less than 40 years of age) AESS Radar Engineer 2010 whose performance is particularly noteworthy as evidenced by contributions to the radar art over a period of several years, with the following citation for “robust CFAR detection, knowledge-based radar signal processing, and waveform design and diversity.” He is the corecipient of the 2013 best paper award (entitled to B. Carlton) of the IEEE Transactions on Aerospace and Electronic Systems with the contribution “Knowledge-Aided (Potentially Cognitive) Transmit Signal and Receive Filter Design in Signal-Dependent Clutter.”